Canadian Conference - Pacific Conference on Earthquake Engineering 2023
Vancouver, British Columbia
June 25th – June 30th, 2023

Performance Evaluation of Weak-Axis Steel Moment Connections

Edgar Tapia-Hernández[1*] and Alejandro Santiago-Flores[3]

[1] Professor - Researcher, Materials Department, Universidad Autónoma Metropolitana, Mexico City.
[2] PhD Student, Universidad Nacional Autónoma de México, Mexico City
[*] *etapiah@azc.uam.mx* (Corresponding Author)

ABSTRACT

During the Puebla earthquake on September 2017 in Mexico, more than 250 steel buildings of different heights were subject to intense shaking. Even though minor structural damage was reported compared to other structural systems, opportunity areas were identified. To establish the vulnerability of existing steel structures, four specimens of beam–column connections with two configurations (two from each) were cyclically tested under quasi-static demands on a natural scale. In particular, weak-axis moment connections (I-beam to the minor axis of the column) were selected since they are commonly employed in steel frames by local practice. From experimental data, tested moment-resisting connections under significant inelastic deformation demands developed an unexpected damage concentration that was not ductile enough for a high-ductility steel structure. In spite of the local Code properly addresses the conceptual requirements, experimental results indicated that studied connections were not as ductile as expected due to the lack of control between the structural design, manufacturing process, and erection. Based on the results, practical recommendations are given for the seismic-resistant design of steel frames with moment connections for new and existing buildings. The envelope curve was obtained to calibrate the inelastic prediction of technical manuals of nonlinear analysis as ASCE 41-2017 and the Mexico City Building Code. This study is part of a research that aims to establish the vulnerability of existing steel structures in Mexico. In addition, experimental data were compared considering a finite element model and detailed models of distributed plasticity in *OpenSees*.

Keywords: Weak-axis steel connection, experimental test, damage concentration, ductility, nonlinear models

INTRODUCTION

Steel moment frames are considered in buildings because of their ductility and energy dissipation capacity under intense seismic demands in the local practice. A complete joint penetration groove weld connection is typically used between the beam and column flange. Because of this, the requirements for the welded unreinforced flange-welded web (WUF-W) connection of the AISC 358-16 Manual are considered. In the WUF-W moment connection, inelastic rotation is developed primarily by yielding at the region adjacent to the flange of the column. The detailing requirements for the welds joining the beam flanges and the beam web to the column flange govern the rupture. The damage is characterized by the beam local buckling, and ductile tearing due to beam buckling as a function of the shape and finish of the weld access holes (AWS D1.8-2016; Han & Kim 2017).

The requirements of beam-to-column steel joints are appropriately addressed in the current version of the local code (MCBC-2020). Nevertheless, due to the lack of control between the structural design, the manufacturing process, and the erection, the designers are not able enough to predict seismic performance. Despite steel moment frames behavior has been studied and adopted in seismic hazard regions, some of the critical issues of beam-to-column moment connections and panel zones are not fully resolved following features of each practice (Tsai y Popov 1989; Han *et al.* 2019). In particular, weak-axis moment connections (I-beam to the minor axis of the column) were studied here since they are commonly employed in steel frames by local practice.

This study aims to contribute to the evaluation of steel buildings with actual connections by following the tendency and conditions of the local market, and considering typical connections. Four beam-column specimens of welded unreinforced flange-welded web (WUF-W) weak-axis moment connections with two configurations (two from each) were cyclically tested. The attention is focused on: *i*) evaluating the inelastic response of the connection of existing structures; *ii*) estimating the inelastic response and the evolution of the damage mechanism of such connections; and *iii*) calibrating nonlinear analytical models.

ESPECIMENS

Two-moment connection solutions to the minor axis of a column I called CTA and CPA (Fig. 1) were studied. In each case, two identical specimens were tested. The seismic performance of beam-to-column weak-axis connection is of interest since, at the local practice, all frames in both directions are usually designed to resist earthquake loading (Tapia-Hernández and García-Carrera 2020). The Specimen CTA (Fig. 1a) is adapted to the weak-column axes following the recommendations of AISC 358-16 for WUF-W. Whereas the Specimen CPA (Fig. 1b) is manufactured by a plate without edges that join the beam to the column's web through stiffener plates. In both cases, the access holes meet the Mexico City Building Code recommendations (MCBC-2020), equivalent to the AWS D1.8 Seismic Supplement (2016). Flanges are welded to the column by full penetration groove welds and have a vertical plate with four bolts used in the assembly process. In addition, the configuration includes stiffener plates at the opposite side of the connection to stiffen the column's web on both sides. Further details about the studied configurations can be found in Santiago-Flores (2021).

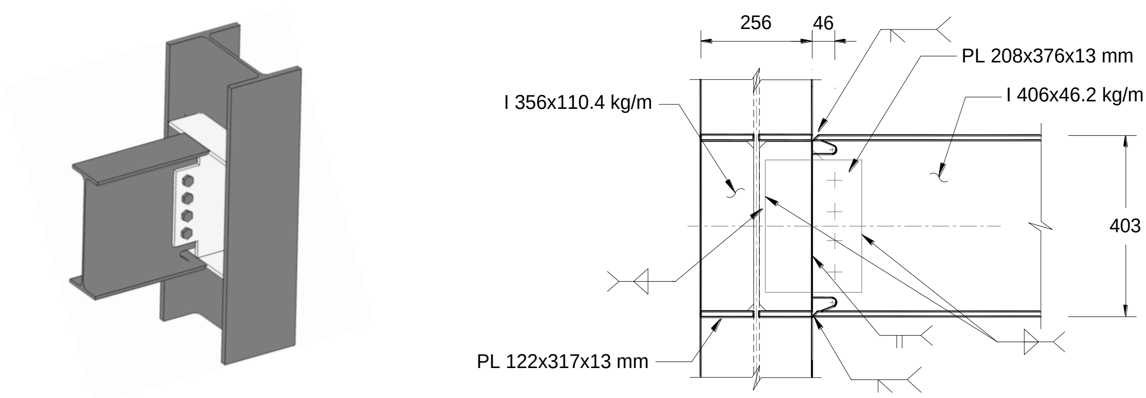

(a)

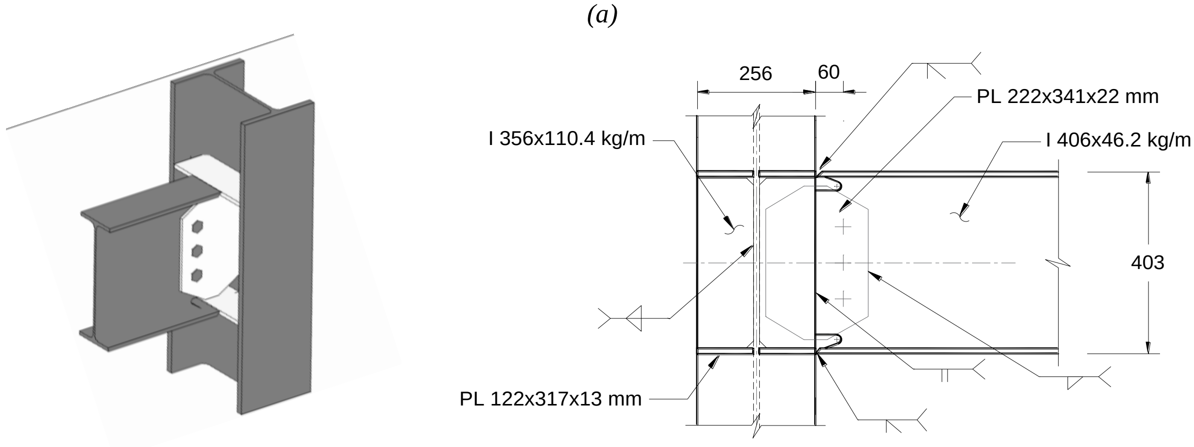

(b)

Fig. 1. Studied configurations: (a) Specimen CTA, (b) Specimen CPA

Studied configurations were identified based on a survey conducted through eleven main design desks and three steelwork fabricators. Welded unreinforced flange-welded web (WUF-W) moment connections were identified as one of the most employed in the latest solutions implemented in new projects. Specimens were constructed by a professional fabricator using certified welders, and all welds had ultrasonically tested by certified inspections following their routine process. All specimens were made from steel ASTM A992/A992M with a tensile yield strength of F_y= 345 MPa (50 kips). Coupon tests were accounted for by computing the actual yield strength at the web and flanges following the ASTM E8/E8M (2016) standard test methods. R_y is the overstrength material factor defined as the ratio between expected F_{ye} and nominal steel yield strength F_y.

Experimental test

In the test, the column was placed horizontally as shown in Fig. 2. A set of angles provided restraint to lateral-torsional buckling perpendicular to the plane of the beam at a distance of 700 mm and 1,500 mm. The experiment was conducted by applying cyclic loads at the top of the cantilever to the vertically mounted specimens through an actuator with capacity of 50 tons. The

AISC 341 (2016) cyclic displacement history was considered based on SAC/BD-97/02 (SAC 1997) for beam-to-column connections. The actuator was anchored to a set of concrete blocks, and it was attached to the beam end in the horizontal direction. The loading sequence was run under displacement control by a quasi-static method.

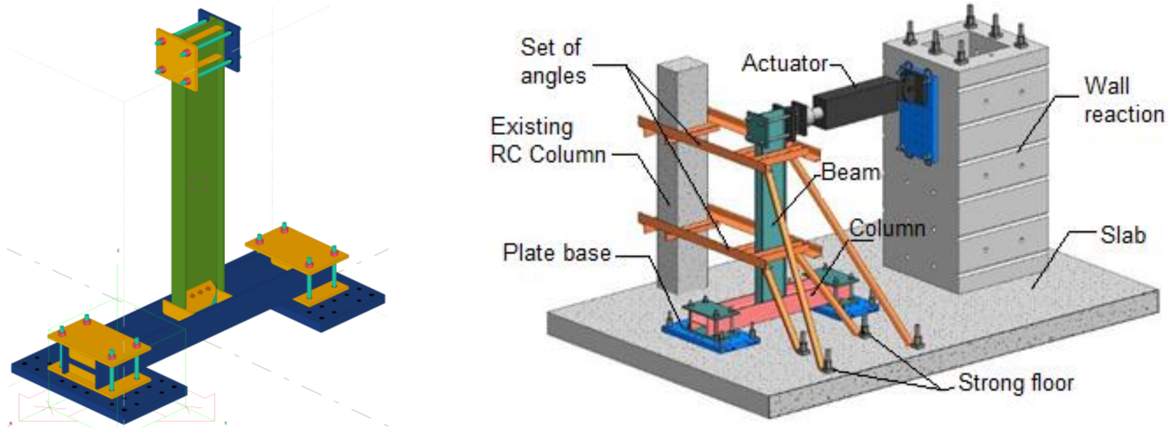

(a) *(b)*

Fig. 2. Configuration, (a) Specimen, (b) Test configuration

DAMAGE EVOLUTION

In tests, the deterioration of the hysteresis curves, which will be discussed later, was caused by local buckling of the beam flange in the access hole zone (Fig. 3). In particular, the deterioration resulting from local buckling is more significant in repeated inelastic cycles such as those that occur under intense seismic demands. Despite this, local buckling could be controlled to develop significant rotational and energy dissipation capacity before fracture, if code requirements are strictly considered.

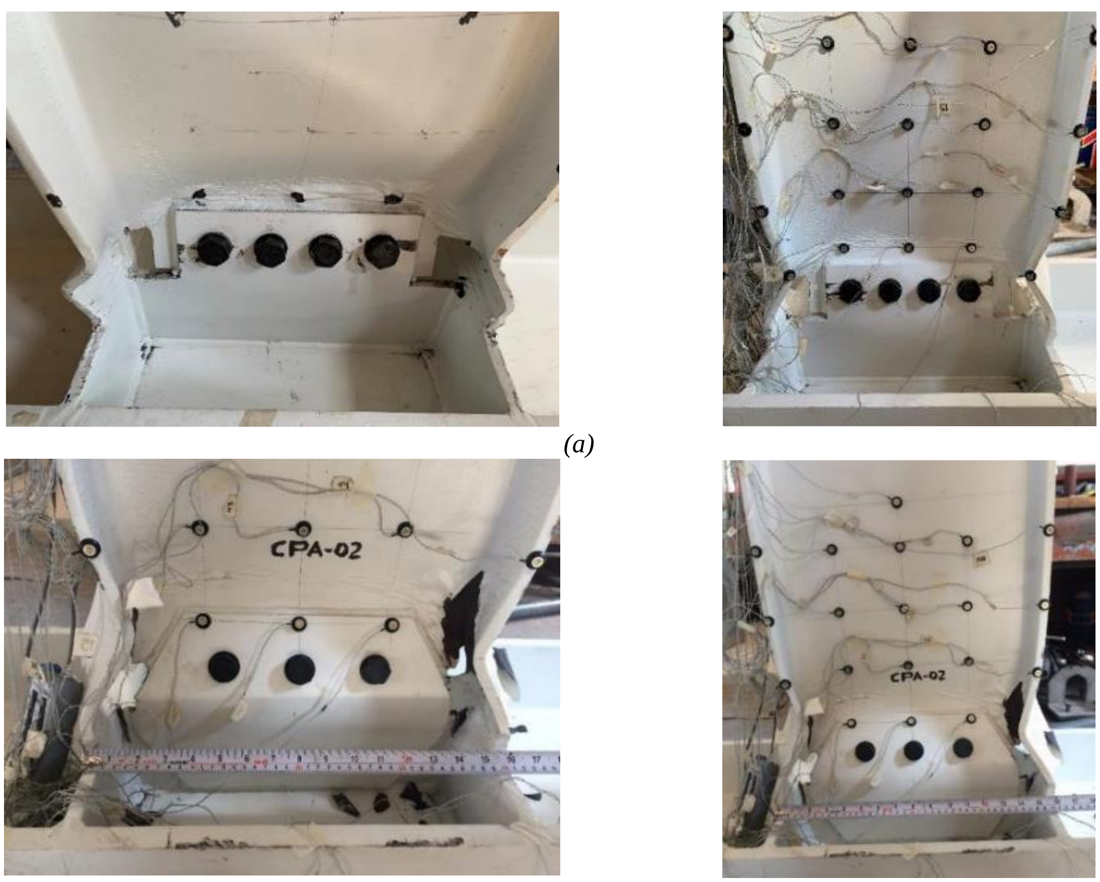

(a)

(b)

Fig. 3. Damage concentration, (a) Typical state of Specimen CTA; (b) Typical state of Specimen CPA

Specimens remained at their load-carrying capacity even when severe damage concentration occurred in either beam flange. In addition, no damage was reported in the column components of any of the specimens. Therefore, the failure was characterized by the local damage at the access hole, and flange local buckling of the beam.

Local slenderness ratios *b/t* are one of the main geometric parameters affecting pre- and post-buckling behavior under seismic demand of steel sections. Maximum plastic rotation achieved from some experimental tests equivalent to those discussed in this research with different slenderness ratios *b/t* are shown in Fig. 4. The requirements for highly ductile members require a ratio *b/t*= 7.23 (*e.g.* AISC 341-16; MCBC-2020) and the minimum angle (γ > 0.04 rad). Thus, the limit of prequalified connections, according to the AISC 358-2016, was included in Fig. 4.

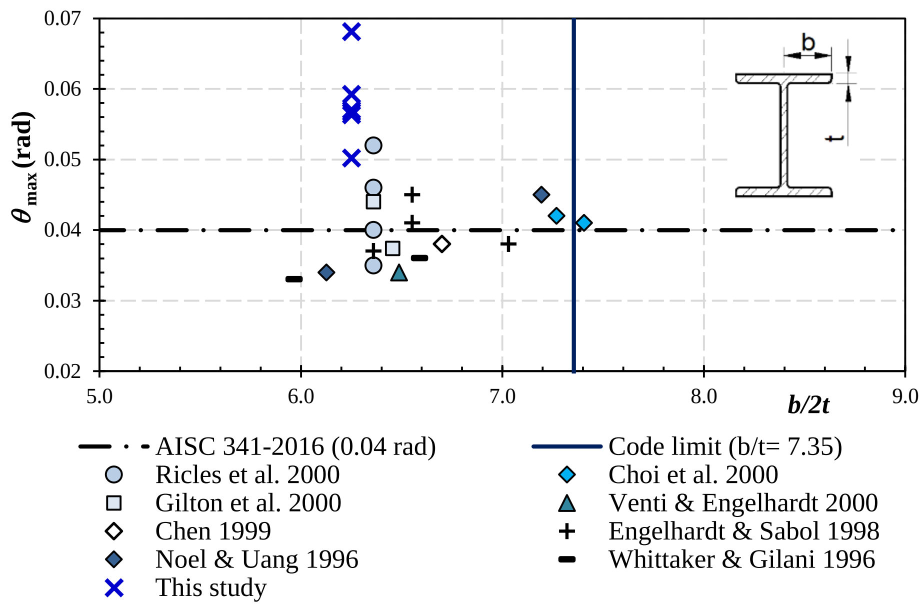

Fig. 4. Plastic rotation as a function of the flange beam slenderness

Based on the results, finite element models were developed to analyze the stress distribution related to local buckling at the beam flange in the tested connections. The finite element model used a three-dimensional solid element for the flanges and web in beam and column elements, reinforcement plates, and panel zone (Fig. 5a). The column was hinged at both ends, and a horizontal load was applied to the end of the beam at the position where the actuator was placed during the experimental tests.

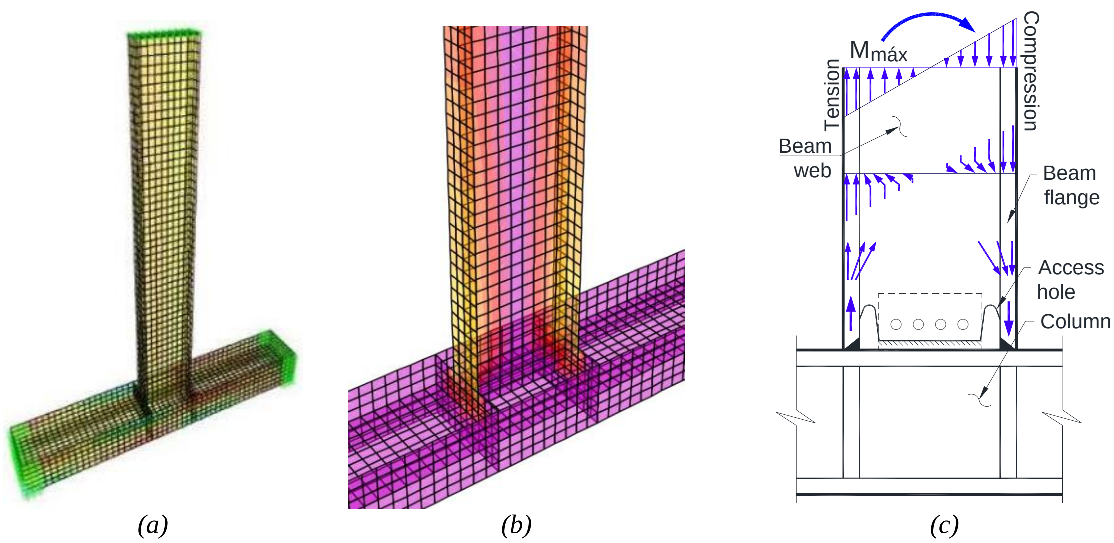

Fig. 5. Analytical model (a) Studied model, (b) Stress distribution, (c) Concentration on flange beam

A static analysis was carried out under incremental monotonic loads to study the stress distribution. Fig. 5b shows the stress distribution associated with a 1.8% drift corresponding to the point where local buckling begins in the flanges. The stress distribution in a color scale reports the maximum in the beam near the access holes. In addition, minor or null damage in the beam's web is reported, which coincides with the response observed in the experimental test (Fig. 3). The forces are concentrated in the beam flanges due to the configuration of the connection. In contrast, the stress distribution is uniform at cross-section when the influence of the connection is neglectable. Thus, local buckling in flanges occurs in response to the application of cyclic loading in the connection in accordance with the stress distribution discussed in Fig. 5c.

HYSTERIC RESPONSE

Fig. 6 shows the hysteresis curves that were obtained in the experimental tests. According to the specialized manuals (*e.g*, AISC 341-2016), the connection used as part of high ductility frames must develop at least 0.04 rad and 80 percent of the plastic moment in a stable way ($0.8M_p$). Based on the above, despite the damage concentration discussed in the previous section, the specimens exceed the plastic moment up to 118 to 121 percent, so that they could be accepted as part of structures with high ductility demands.

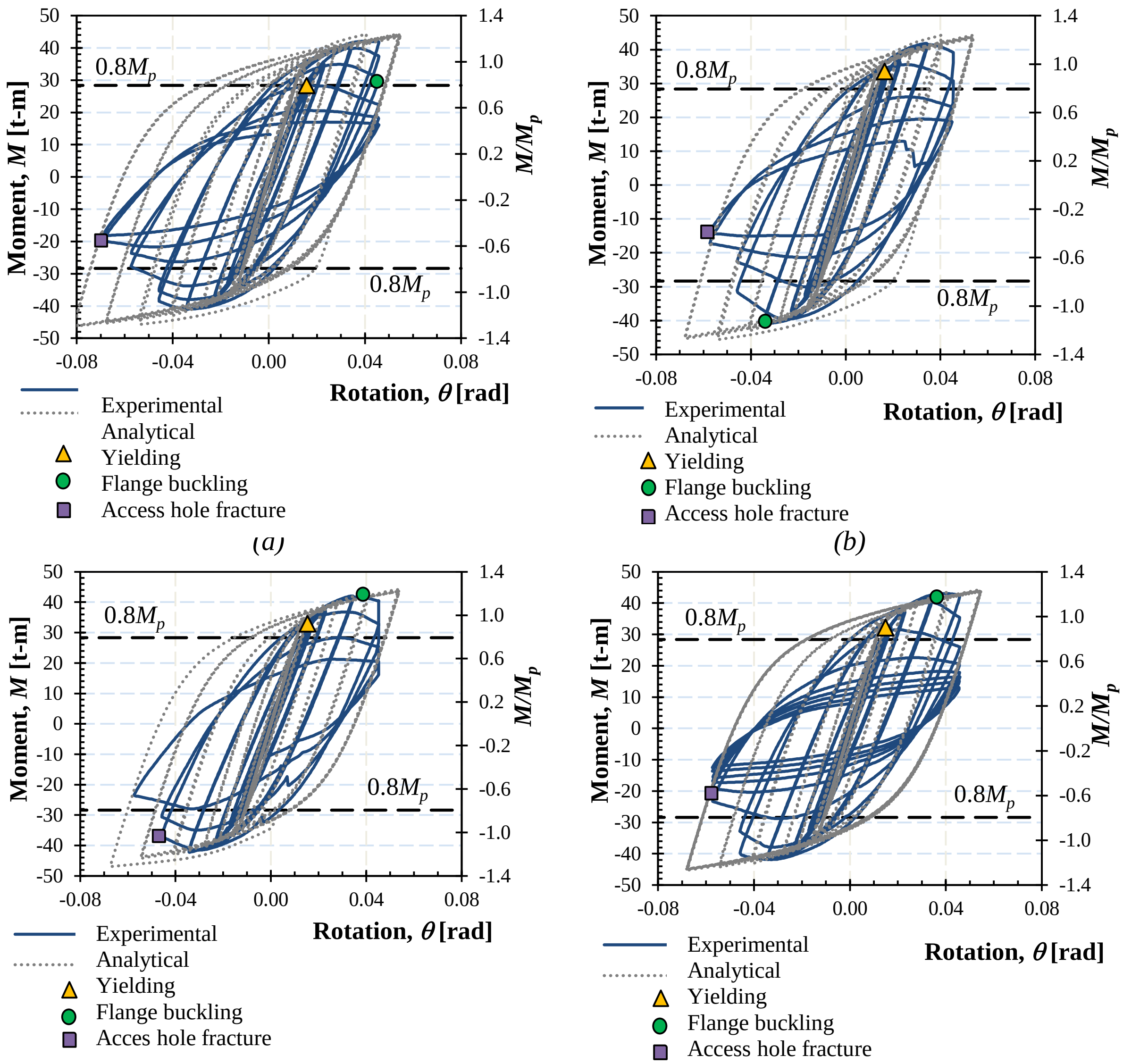

Fig. 6. Hysteretic curves (a) Specimen CTA-1; (b) Specimen CTA-2; (c) Specimen CPA-1;(d) Specimen CPA-2

The hysteresis curves identify the evolution of the damage considering three states:

i. Yielding. During the experimental test, some fibers of the cross-section yield ($f > F_y$) in this state, but it does not mean that the section has yielded. For this reason, the structural section has no physical damage, although the instruments begin to report an inelastic response.
ii. Flange buckling. It refers to the physical state where the flange beam began to buckle and which was discussed extensively in the previous section.
iii. Hole access fracture. Refers to the point where a crack propagated into the web beam from the hole access. This fracture was related to a sudden degradation of resistance that made it necessary to stop the test.

ANALYTICAL MODEL

Detailed analytical models were developed in *OpenSees* (Mazzoni *et al*., 2006). Nonlinear static analysis was performed to determine the maximum probable load and displacement. In addition, nonlinear hysteretic analyzes were performed by applying the same displacement protocol as the experimental test to compare the behavior of the connection under cyclic loads.

To define the geometry of the model, the central lines of the elements were considered, as shown in Fig. 7. Nonlinear elements with plasticity distributed along the length of the element were considered for beam and column members. Three rectangular sections were used to generate the cross-section of each member: one for the web and two for each flange (Fig. 7a). The sections were discretized into quadrilateral-shaped fibers with four integration points per element. The analytical model was constructed from previous parametric studies (Tapia *et al.* 2016; Tapia and García 2019).

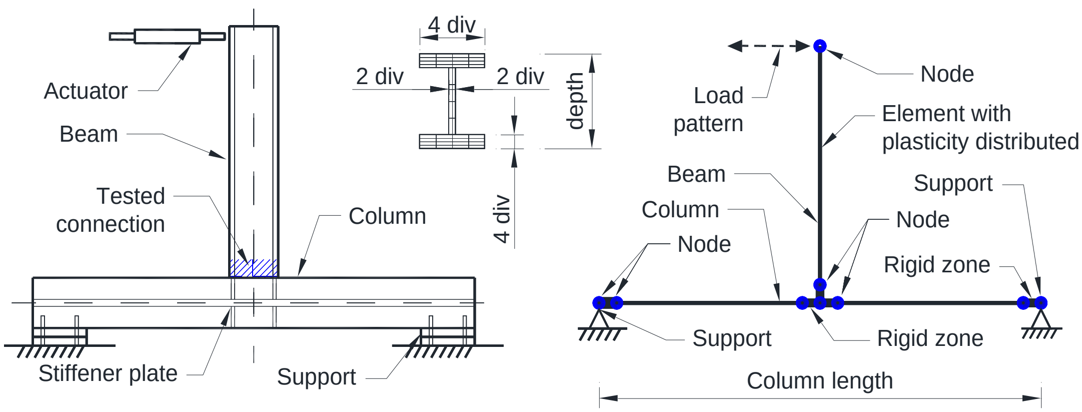

(a) Specimen elevation *(b) Analytical model*

Fig. 7. Studied model characteristics

The material was defined through the Giufre-Menegotto-Pinto (GMP) uniaxial model for fibers, which includes isotropic and kinematic strain hardening. The model analyzes the response along the member by integrating the uniaxial hysteretic model over the section. Finally, the column was pinned at both ends, and the load was applied to the end of the beam at the actuator's position, as depicted in Fig. 7b.

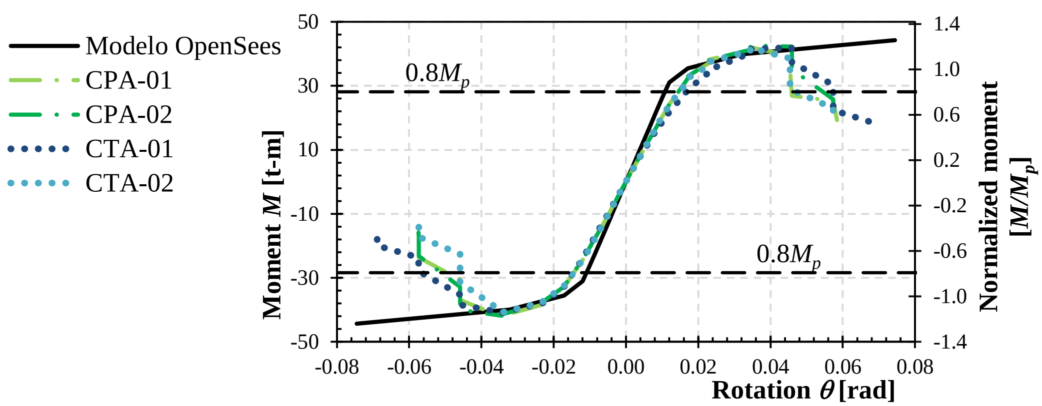

Fig. 8. Capacity curve and enveloped experimental response

To calibrate the analytical model, a static analysis was first carried out under incremental monotonous loads, which was compared against the enveloping curves of the obtained hysterical response (Fig. 8). For this purpose, enveloping curves were drawn extracting the maximum moments from the test at each cycle. The analytical model reports a slightly higher initial stiffness. This tendency is common when analytical studies are compared with experimental tests, and it is explained because the model does not perfectly include all possible physical sources of deformation and slight displacements between the components of the specimen. Despite this, the model seems to be an adequate representation of the experimental response of the connections.

A nonlinear dynamic analysis was carried out, where the displacement protocols used in the experimental test were applied. The cyclical analysis was based on the load pattern and time from a series of discrete points in space with the Path TimeSeries command (Mazzoni *et al.*, 2006). The results were compared with the hysteresis curve (momentum - rotation) obtained in the experimental test, as also shown in Fig. 6.

The analytical results adequately represent the response in the elastic range and capture the beginning of stiffness and strength degradation. Stable hysteresis loops and repeatable power dissipation are observed over a large number of cycles. Because the analytical method cannot capture local buckling and fracture degradation, the curves differ significantly for higher hysterical cycles with strength and stiffness degradation, which explains the differences when specimen damage is significant. However, the results confirm that the connection is reliable to achieve an inelastic rotation of 0.04 rad or greater before failure.

Analysis parameters and acceptance criteria

The required strength for ductile structures to be at least $0.8M_p$ is established, intending that structures be stressed to a magnitude prior to strength degradation (AISC 341-16). With this, an attempt is made to prevent collapses in the face of intense seismic demands; based on a probabilistic function that the resistance degradation occurs when the deformation in 0.04 rad meets those performance objectives (FEMA 356, 2000). However, the earthquake-resistant design approach has evolved. Social expectations after an intense earthquake are based not only on the state of collapse prevention but also on the design of sustainable and resilient structures.

For this reason, the behavior of the structures is evaluated from analysis procedures and acceptance criteria based on the inelastic response. In particular, ASCE 41 (2017) defines parameters for analytical models based on experimental tests that support the inelastic behavior of elements subjected to cyclic loads.

Based on the procedure, idealized force-deformation curves were calculated from the experimental data obtained to compare performance levels. The enveloping curve was determined as the average of the experimental results, calculated as a series of linear segments. In Fig. 9, the envelope curves of the four specimens and the average envelope curve are shown as a thicker black solid line. Based on the results, the envelopes are essentially the same, up to 0.035 rad, associated with Life Safety (SV) strength degradation. From this deformation demand, the curves differ depending on the damage sequence reported in each test. The average envelope curve obtained corresponds to a ductile element defined in the specialized codes (ASCE 41-2017, MCBC-2020) with:

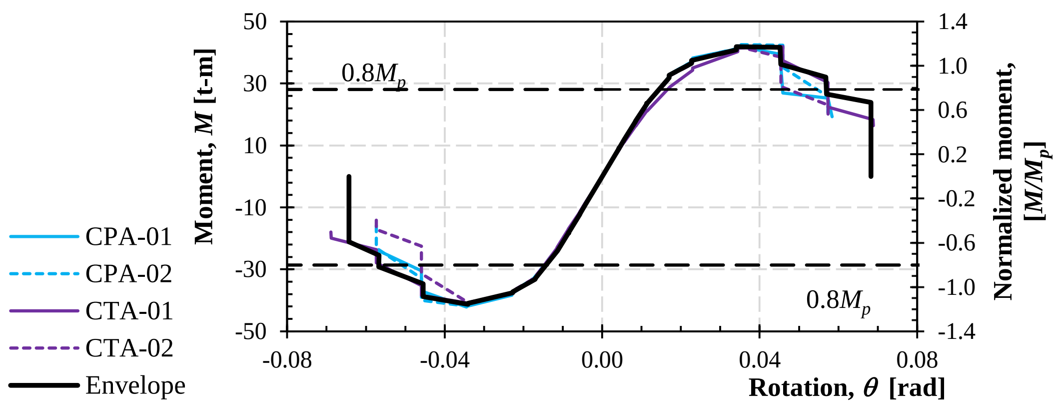

Fig. 9. Envelopes of the experimental test

Fig. 10 compares the envelope obtained from the experimental tests, the curves proposed by the ASCE 41-13 and ASCE 41-17 manual for beams dominated by bending effects, and the criteria for welded unreinforced flange-welded web connections, such as those discussed in this investigation. Additionally, the performance levels proposed for each case are included, where the Immediate Operation (IO) level is the same in all cases.

The linear response (effective flexural stiffness K_e) is stiffer in the analytical approaches. Therefore, the ductility expectation of the connection may be greater than that which the plastic hinge could develop under actual conditions. In addition, it is noted that a 3% slope fits the strain hardening reported in the experimental test. According to the results, the manual criteria for WUF connections tend to underestimate the deformation capacity of the maximum resistance by 0.84 times. In contrast, it was identified that the enveloping curve of the experimental tests has a better coincidence with the criteria of the ASCE 41-13 manual for beams, where the contribution of shear deformation is not included.

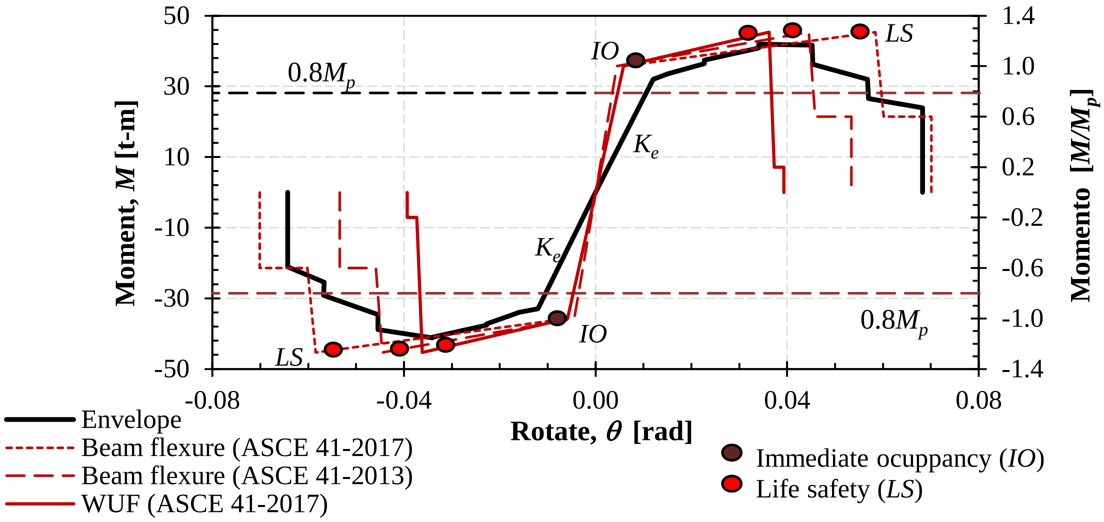

Fig. 10. Idealized force-displacement curves and enveloping curve

Experiments suggest that the ASCE 41-2013 and 2017 nonlinear component models do not accurately represent the expected connection behavior under cyclic loading following a lumped plasticity model. This observation underlines the relevance of carrying out experimental tests of existing building connections. In any case, the deterioration of the resistance of the envelope is related to a level of Safety of Life (SV) performance in the idealized force-displacement curves. Given the accumulated damage in the connections, the current criteria based on the control of resistance degradation ($0.8M_p$; 0.04 rad) might not be appropriate for the studied connection, especially when considering societal expectations of resilience. Although the beams and columns will remain elastic for that level of damage ($0.8M_p$; 0.04 rad), the building would be unoccupied and subject to a deep rehabilitation process.

CONCLUSIONS

The results of an analytical and experimental investigation of the behavior of existing connections in steel buildings in Mexico are discussed in this paper. The attention is focused on the seismic response of two configurations of I-beam steel connections to the weak axis of the column. Quasi-static experimental tests were carried out on a full scale. The specimen configurations were established through surveys among some of the most important design firms and steel structure manufacturers. In each case, two specimens were tested to study the evolution of damage from the experimental test. The main contributions of this research are the following:

- The failure in the specimens was led by the buckling of the flanges in the area of the weld access hole, which evolved into a stress concentration, even though the specimens satisfy the requirements for compact sections. Consequently, the connections report a decrease in the inelastic response, which could be avoided by strictly applying the geometric and roughness recommendations for the access hole of current regulations. In fact, according to the plans, all the access holes for welding had to comply with the normative details and tolerances; however, the final product needed to be more precise, revealing an inaccuracy between the structural design, manufacturing process, and assembly.
- Despite the damage concentration, the connections were able to meet the requirements of resistance 0.8Mp and deformation 0.04 rad to be considered as part of frames with a high demand for ductility. However, it was underlined that these limits were established in relation to the maximum strength as a method of avoiding collapse, which is different from the resilience expectations of current seismic design approaches. The conceptual understanding of lateral deformations and their relationship to the damage mechanism and its implications was highlighted.
- Analytical models were carried out in the *OpenSees*, which adequately estimate the behavior of the specimens when the deformation demand is controlled (0.035 rad) in terms of resistance and stiffness. However, the analytical results differ for higher cycles, given the evolution of the damage in each particular case.
- The enveloping curve of the experimental tests was obtained and compared with the criteria of current regulations for the prediction of inelastic response. Experiments suggest that the ASCE 41-2013 and 2017 nonlinear component models do not accurately represent the expected connection behavior under cyclic loading following a lumped plasticity model. This observation underlines the relevance of carrying out experimental tests, especially, of existing building connections.

REFERENCES

[1] AISC-341 (2016), *Seismic Provisions for Structural Steel Buildings*, ANSI/AISC 341-16. American Institute of Steel Construction. Chicago, IL, United States.

[2] AISC-358 (2016), *Prequalified Connections for Special and Intermediate Steel Moment Frames for Seismic Applications*, ANSI/AISC 358-16. American Institute of Steel Construction. Chicago, IL, United States.

[3] ASCE 41 (2013), *Seismic Evaluation and Retrofit of Existing Buildings*, Standard ASCE/SEI 41-13, American Society of Civil Engineers. Reston, VA, United States.

[4] ASCE 41 (2017), *Seismic Evaluation and Retrofit of Existing Buildings*, Standard ASCE/SEI 41-17, American Society of Civil Engineers. Reston, VA, United States.

[5] ASTM E8/E8M (2016), *Standard Test Methods for Tension Testing of Metallic Materials*, American Society for Testing and Materials, ASTM, American National Standard, West Conshohocken, PA, United States.

[6] AWS D1.8 (2016), *Structural Welding Code – Seismic Supplement*, An American National Standard, AWS D1.8/D1.8 M, American Welding Society D1 Committee on Structural Welding, 3a edición.

[7] Chen, S.J. (1999), "Design of Ductile Steel Beam-to-Column Connections for Seismic Resistance," *Workshop on Design Technologies of Earthquake-Resistant Moment Resisting Connections*, Taipei, Taiwan.

[8] Choi, J., Stojadinovic, B., and Goel, S.C. (2000), Parametric Tests on the Free Flange Connection, *Report SAC/BD-00/02*, SAC Joint Venture.

[9] Engelhardt M.D. y Sabol T.A. (1998), "Reinforcing of Steel Moment Connections with Cover Plates: Benefits and Limitations", *Engineering Structures*, Vol. 20, No. 4-6, pp. 510-20, Elsevier, London.

[10] FEMA 356 (2000), "Prestandard and commentary for the seismic rehabilitation of buildings", prepared by the *American Society of Civil Engineers for the Federal Emergency Management Agency*. Washington, D.C. United States of America. November.

[11] Gilton C.S., Chi, B. y Uang C.M. (2000), "Cyclic Testing of a Free Flange Moment Connection", *SAC Report 00/19*, SAC Joint Venture.

[12] Han S.W. & Kim N.H. (2017), Permissible parameter ranges of access hole geometries for WUF-W Connections, Earthquake Spectra, Vol. 33, Issue 2, Pp. 687-707

[13] Han S.W., Moon K.H. & Jung J. (2019). Cyclic Performance of Welded Unreinforced Flange-Welded Web Moment Connections, Earthquake Spectra, Volume 30, Issue 4. Pp. 1663-1681.

[14] Mazzoni, S., F. McKenna, M. Scott, M y G. Fenves (2006). Open system for earthquake engineering simulation, user command-language manual, Report NEES grid-TR 2004-21. *Pacific Earthquake Engineering Research*, University of California, Berkeley, CA.

[15] MCBC-2020 (2020), Mexico City Building Code, Gaceta Oficial de la Ciudad de México. Mexico (in Spanish).

[16] Noel S. y Uang C.M. (1996), "Cyclic Testing of Steel Moment Connections for the San Francisco Civic Center Complex", Report TR-96/07, *Division of Structural Engineering*, U. of California, San Diego, CA.

[17] Ricles J.M., Mao C., Lu L.W. y Fisher J.W. (2000), "Development and Evaluation of Improved Details for Ductile Welded Unreinforced Flange Connections", *SAC BD 00-24*, SAC Joint Venture.

[18] SAC (1997), "Interim Guideless Advisory No. 1: Supplement to FEMA 267. Program to Reduce the Earthquake Hazards of Steel Moment Frame Structures. Federal Emergency Management Agency. Report FEMA 267A/SAC-96-03. SAC Joint Venture. Sacramento, California.

[19] Santiago-Flores A. (2021), "Behavior of connection of steel frames under seismic demands", Master Thesis, Universidad Nacional Autónoma de México (In Spanish).

[20] Tapia E, García J.S. y Del Rincón A., (2016), "Estudio paramétrico del modelado inelástico de contravientos de acero", *Revista de Ingeniería Sísmica, SMIS.* No. 94. Pp. 49-74. *doi: dx.doi.org/10.18867/ris-0*

[21] Tapia E. y García J.S., (2019), "Inelastic response of ductile eccentrically braced frames", *Journal of Building Engineering*, No. 25. *https://doi.org/10.1016/j.jobe.2019.100903*

[22] Tapia-Hernández E. y García-Carrera J.S. (2020), "Damage assessment and Seismic behavior of Steel Buildings during the Mexico Earthquake of September 19, 2017". Earthquake Spectra. Vol. 36, Issue 1.

[23] Tsai, K. C. y Popov, E. P. (1989). Steel Beam-Column Joints in Seismic Moment Resisting Frames. Rep. No. UCBIEERC 88/19, Earthquake Engineering Research Center, Universidad de California, Berkeley, California. Estados Unidos.

[24] Venti M. y Engelhardt M.D. (2000), "Test of a Free Flange Connection with a Composite Floor Slab", *SAC Report 00/18*, SAC Joint Venture.

[25] Whittaker A.S. & Gilani A. (1996), "Washington High School Reconstruction - Cyclic Testing of Steel Beam-Column Connections", Report No. EERCL-STI/96-04, *Earthquake Engineering Research Center*, University of California, Berkeley, CA.